

PLASTIC ANALYSIS OF MIXED MODE PLANE
STRESS CRACK PROBLEMS*

J. W. Hutchinson and C. F. Shih
Harvard University, Cambridge, Massachusetts 02138

ABSTRACT

Two parameters are identified for characterizing the deformation in the plastic zone near the tip of a crack when mixed mode conditions prevail. Details of the near-tip stress and strain distributions are presented for hardening materials in which a diffuse plastic zone occurs under plane stress conditions. For small scale yielding the two near-tip parameters are related to the two elastic stress intensity factors for combined Mode I and Mode II.

PLASTIC STRESS AND STRAIN FIELDS FOR MIXED MODE CRACK PROBLEMS

Solutions to two dimensional crack problems in the plane for isotropic elasticity are characterized by the near-tip stress distribution

$$\sigma_{ij} = (2\pi r)^{-1/2} [K_I \sigma_{ij}^I(\theta) + K_{II} \sigma_{ij}^{II}(\theta)] , \quad (1)$$

where r and θ are planar polar coordinates such that $\theta = 0$ directly ahead of the crack. The θ -variation of the Mode I contribution to the stresses is symmetric with respect to the crack tip while the Mode II contribution is antisymmetric. Mode I and II elastic stress intensity factors, K_I and K_{II} , constitute a two parameter characterization of the elastic

PLASTIC STRESS AND STRAIN FIELDS FOR MIXED MODE CRACK PROBLEMS

Solutions to two dimensional crack problems in the plane for isotropic elasticity are characterized by the near-tip stress distribution

$$\sigma_{ij} = (2\pi r)^{-1/2} [K_I \sigma_{ij}^I(\theta) + K_{II} \sigma_{ij}^{II}(\theta)] , \quad (1)$$

where r and θ are planar polar coordinates such that $\theta = 0$ directly ahead of the crack. The θ -variation of the Mode I contribution to the stresses is symmetric with respect to the crack tip while the Mode II contribution is antisymmetric. Mode I and II elastic stress intensity factors, K_I and K_{II} , constitute a two parameter characterization of the elastic near-tip field.

For two dimensional crack problems in which the material is modeled by a deformation theory of plasticity and in which the equilibrium equations and strain-displacement relations are taken to be linear, it can be shown that the strain energy density must vary like $1/r$ as the crack tip is approached

Here σ_0 is a reference stress which can be identified with the tensile yield stress if convenient, E is Young's modulus, n is the hardening exponent and α is a material constant. In this case the dominant singularity fields are of the form

$$\sigma_{ij} \sim r^{-1/(n+1)} \tilde{\sigma}_{ij}(\theta) \quad \text{and} \quad \epsilon_{ij}^P \sim r^{-n/(n+1)} \tilde{\epsilon}_{ij}^P(\theta) . \quad (3)$$

Details of these fields have been given for the pure modes in [1, 2, 3]. The θ -variations $\tilde{\sigma}_{ij}$ and $\tilde{\epsilon}_{ij}^P$ depend implicitly on n and, in contrast to linearly elastic problems, depend in a significant way on whether plane stress or plane strain pertains.

The mixed mode crack tip fields for linear elasticity (1) are simply the superposition of the Mode I and Mode II contributions. The plasticity problem is inherently nonlinear so that a representation such as (1) cannot be used. As a measure of the relative amounts of Mode I and Mode II at the crack tip we introduce a near-tip mixity parameter M^P defined by

$$M^P = \frac{2}{\pi} \tan^{-1} \left| \lim_{r \rightarrow 0} \frac{\sigma_{\theta\theta}(r, \theta = 0)}{\sigma_{r\theta}(r, \theta = 0)} \right| . \quad (4)$$

With this choice M^P ranges from $M^P = 0$ for pure Mode II to $M^P = 1$ for pure Mode I.

The simplest deformation theory, J_2 deformation theory, has been used to generalize (2) to multiaxial states of stress. It is convenient to introduce the effective stress σ_e where $\sigma_e^2 = 3s_{ij}s_{ij}/2$ and $s_{ij} = \sigma_{ij} - \sigma_{pp}\delta_{ij}/3$. The near-tip fields can be represented in the form

crack tip we introduce a near-tip mixity parameter M^P defined by

$$M^P = \frac{2}{\pi} \tan^{-1} \left| \lim_{r \rightarrow 0} \frac{\sigma_{\theta\theta}(r, \theta = 0)}{\sigma_{r\theta}(r, \theta = 0)} \right| . \quad (4)$$

With this choice M^P ranges from $M^P = 0$ for pure Mode II to $M^P = 1$ for pure Mode I.

The simplest deformation theory, J_2 deformation theory, has been used to generalize (2) to multiaxial states of stress. It is convenient to introduce the effective stress σ_e where $\sigma_e^2 = 3s_{ij}s_{ij}/2$ and $s_{ij} = \sigma_{ij} - \sigma_{pp}\delta_{ij}/3$. The near-tip fields can be represented in the form

$$\begin{aligned} [\sigma_{ij}, \sigma_e] &= \sigma_0 K_M^P r^{-1/(n+1)} [\tilde{\sigma}_{ij}(\theta, M^P), \tilde{\sigma}_e(\theta, M^P)] \\ \epsilon_{ij}^P &= (\alpha\sigma_0/E)(K_M^P)^n r^{-n/(n+1)} \tilde{\epsilon}_{ij}^P(\theta, M^P) . \end{aligned} \quad (5)$$

The plastic stress intensity factor K_M^P can be thought of as

$\tilde{\sigma}_e^2 = 3\tilde{s}_{ij}\tilde{s}_{ij}/2$ and $\tilde{s}_{ij} = \tilde{\sigma}_{ij} - \tilde{\sigma}_{pp}\delta_{ij}/3$. For a given value of n and for either plane stress or plane strain conditions, the functions $\tilde{\sigma}_{ij}$, $\tilde{\sigma}_e$ and $\tilde{\epsilon}_{ij}^P$ are completely specified by the mixity parameter M^P . Details of these functions have been given for the case of plane strain in [4]; plane stress results will be discussed below.

Once the hardening exponent n is specified, K_M^P and M^P completely characterize the near-tip field. In place of the combination (K_M^P, M^P) it may be more convenient to introduce the path independent J integral [5] and to use the equivalent pair (J, M^P) . The three parameters are connected by [1]

$$J = (\alpha\sigma_0^2/E)I_n(M^P)(K_M^P)^{n+1}, \quad (6)$$

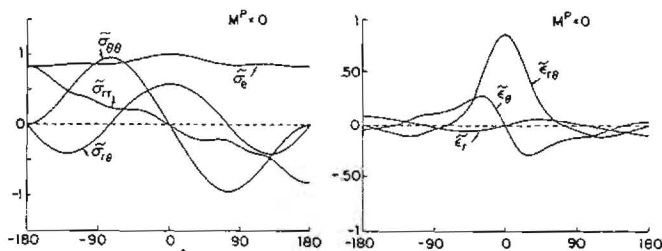
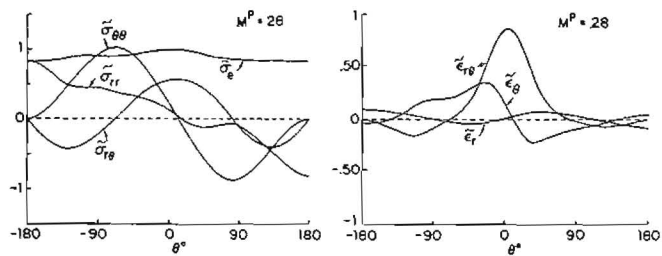
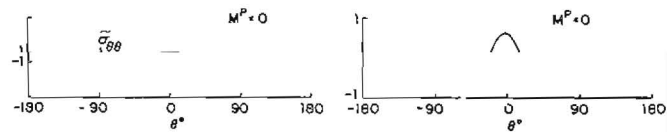
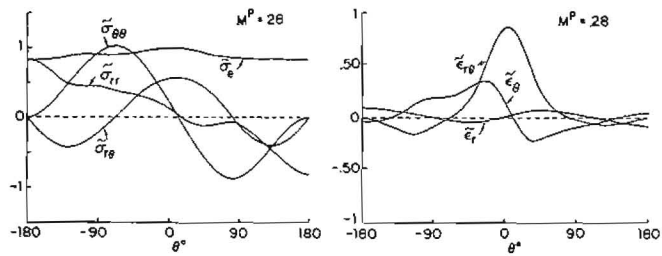
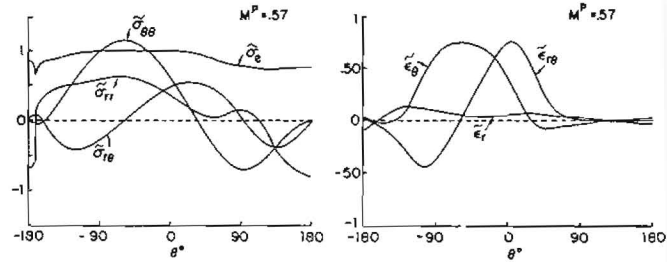
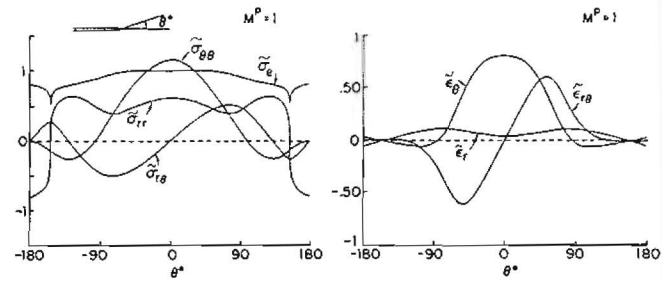
where I_n is a numerical constant determined from the singularity analysis which depends on n and M^P . Plane strain values of I_n where given in [4] and plane stress values will be given below. In the pure mode cases M^P is known and thus J (or equivalently K_M^P) is a single parameter measuring the intensity of deformation in the near-tip field. But in the general mixed mode situation a pair of parameters is needed for a complete characterization.

PLANE STRESS NEAR-TIP FIELDS

Figure 1 gives the θ -variations of the stresses and strains in (5) for a relatively low strain hardening material with $n=13$. Pure Mode I and pure Mode II are included along with two intermediate cases. The plane stress formulation used here is the same as employed in the Mode I study in [1]. It does not take into account the nonlinear geometric effect arising from sheet thinning. This, together with the assumption of a hardening material, leads to a diffuse plastic zone as opposed to the slender necking zone represented by the Dugdale model. Numerical methods used to calculate these quantities are discussed in [4] and in more detail in [6].

PLANE STRESS NEAR-TIP FIELDS

Figure 1 gives the θ -variations of the stresses and strains in (5) for a relatively low strain hardening material with $n=13$. Pure Mode I and pure Mode II are included along with two intermediate cases. The plane stress formulation used here is the same as employed in the Mode I study in [1]. It does not take into account the nonlinear geometric effect arising from sheet thinning. This, together with the assumption of a hardening material, leads to a diffuse plastic zone as opposed to the slender necking zone represented by the Dugdale model. Numerical methods used to calculate these quantities are discussed in [4] and in more detail in [6].



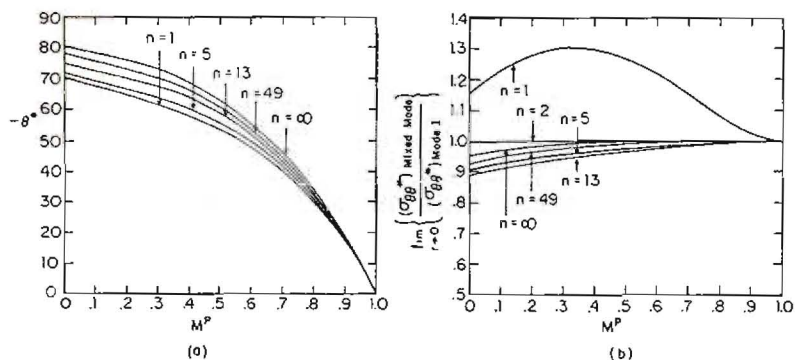


Fig. 2 (a) Angular position of maximum tensile stress θ^* (in degrees) as a function of the near-tip mixity parameter. (b) Ratio of the amplitude of the maximum tensile stress in mixed mode to that in Mode I for identical values of J .

The value of this maximum stress is normalized by the corresponding Mode I value, $\sigma_{\theta\theta}(\theta=0)$, at the same r and same value of J . This ratio is shown as a function of M^P in Fig. 2b. Analogous curves for plane strain in [4] indicate a significant fall-off in the maximum tensile stress amplitude away from Mode I which is absent in plane stress.

Values of I_n , which enter into (6), are given in the form of curves in Fig. 3.

SMALL SCALE YIELDING

In the small scale yielding limit, when, roughly speaking, the plastic zone is small compared to the crack length and $\sigma_{\theta\theta}^*$ is small compared to the yield stress, σ_y , the ratio of the maximum tensile stress in mixed mode to that in Mode I for identical values of J .

The value of this maximum stress is normalized by the corresponding Mode I value, $\sigma_{\theta\theta}(\theta=0)$, at the same r and same value of J . This ratio is shown as a function of M^P in Fig. 2b. Analogous curves for plane strain in [4] indicate a significant fall-off in the maximum tensile stress amplitude away from Mode I which is absent in plane stress.

Values of I_n , which enter into (6), are given in the form of curves in Fig. 3.

SMALL SCALE YIELDING

In the small scale yielding limit, when, roughly speaking, the plastic zone is small compared to the crack length and all other relevant geometric lengths, J can be expressed in terms of the elastic stress intensity factors according to (for plane stress [5])

$$J = (K_I^2 + K_{II}^2)/E. \quad (7)$$

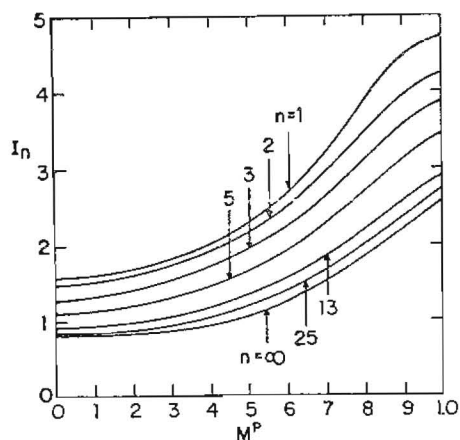


Fig. 3 Values of $I_n(M^p)$.

$$M^e = \frac{2}{\pi} \tan^{-1} \left| \lim_{r \rightarrow 0} \frac{\sigma_{\theta\theta}(r, \theta = 0)}{\sigma_{r\theta}(r, \theta = 0)} \right| = \frac{2}{\pi} \tan^{-1} \left| \frac{K_I}{K_{II}} \right|. \quad (8)$$

(For a crack in an infinite sheet making an angle β (in radians) to a far pure tension field, $M^e = 2\beta/\pi$.) Either pair, (K_I, K_{II}) or (J, M^e) , completely specifies the near-tip field of the elastic mixed mode solution.

The results of the numerical analysis of the small scale yielding problem are shown in Fig. 4a in the form of plots of M^p as a function of M^e for various n . The curve labeled

Fig. 3 Values of $I_n(M^p)$.

$$M^e = \frac{2}{\pi} \tan^{-1} \left| \lim_{r \rightarrow 0} \frac{\sigma_{\theta\theta}(r, \theta = 0)}{\sigma_{r\theta}(r, \theta = 0)} \right| = \frac{2}{\pi} \tan^{-1} \left| \frac{K_I}{K_{II}} \right|. \quad (8)$$

(For a crack in an infinite sheet making an angle β (in radians) to a far pure tension field, $M^e = 2\beta/\pi$.) Either pair, (K_I, K_{II}) or (J, M^e) , completely specifies the near-tip field of the elastic mixed mode solution.

The results of the numerical analysis of the small scale yielding problem are shown in Fig. 4a in the form of plots of M^p as a function of M^e for various n . The curve labeled $n = \infty$ was obtained by extrapolation. The functional relation between M^p and M^e in plane stress small scale yielding is independent of Poisson's ratio and the amplitude of the singularity. It does depend implicitly on other shape details of the uniaxial stress-strain curve in addition to n . The results of Fig. 4 were obtained using the tensile relation

$\epsilon/\epsilon_s = \sigma/\sigma_s$ for $\sigma < \sigma_s$ and $\epsilon/\epsilon_s = (\sigma/\sigma_s)^n$ for $\sigma > \sigma_s$,

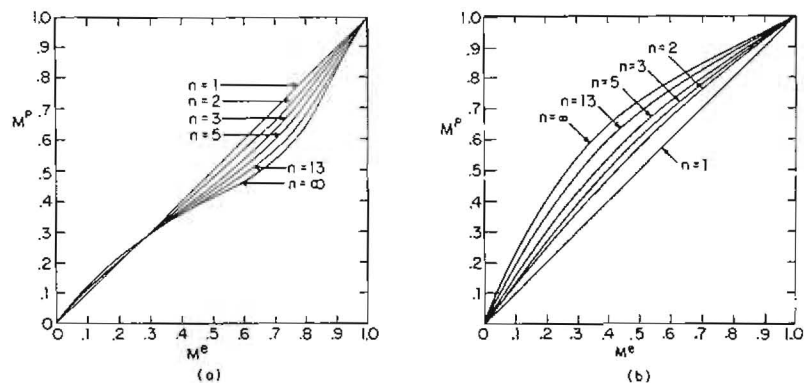


Fig. 4 Near-tip mixity M^P as a function of M^e for small scale yielding. (a) plane stress, (b) plane strain for $\nu=0.3$ from [4].

The results of Fig. 2 may be reexpressed in terms of M^e using the connection between M^P and M^e . Thus, Fig. 5a shows the effect of the hardening exponent on the critical angle θ^* as a function of the elastic mixity parameter for small scale yielding in plane stress. The curves for plane strain from [4] are shown in Fig. 5b along with some experimental data on fracture initiation angles from [7, 8]. According to the plasticity analysis, a fairly wide range of fracture initiation angles about the elastic prediction ($n=1$) should be expected depending on the hardening exponent and on whether the plane stress or plane strain condition is approached.

Plastic zones for small scale yielding in plane stress are shown in Fig. 6 for four values of mixity. (a) plane stress, (b) plane strain for $\nu=0.3$ from [4].

The results of Fig. 2 may be reexpressed in terms of M^e using the connection between M^P and M^e . Thus, Fig. 5a shows the effect of the hardening exponent on the critical angle θ^* as a function of the elastic mixity parameter for small scale yielding in plane stress. The curves for plane strain from [4] are shown in Fig. 5b along with some experimental data on fracture initiation angles from [7, 8]. According to the plasticity analysis, a fairly wide range of fracture initiation angles about the elastic prediction ($n=1$) should be expected depending on the hardening exponent and on whether the plane stress or plane strain condition is approached.

Plastic zones for small scale yielding in plane stress are shown in Fig. 6 for four values of mixity. These zones were calculated using the power hardening law for uniaxial tension stated above. Mode I zones have been given earlier in [9] and are similar to those shown in Fig. 6 for $M^e=1$, except that the present zones extend somewhat further ahead of the crack. It is felt that the present calculations are more accurate than those reported in [9].

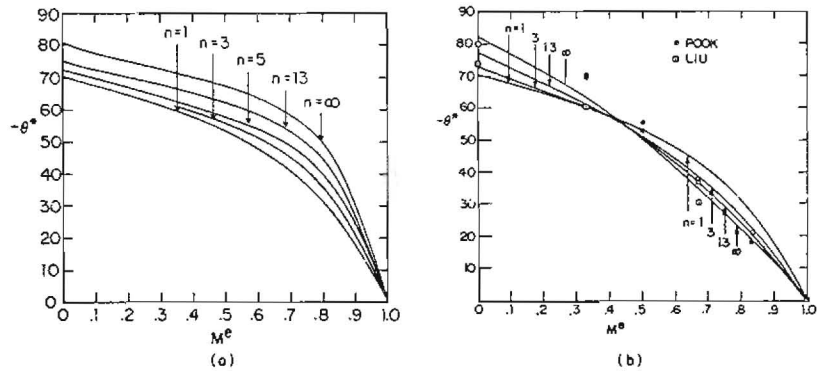
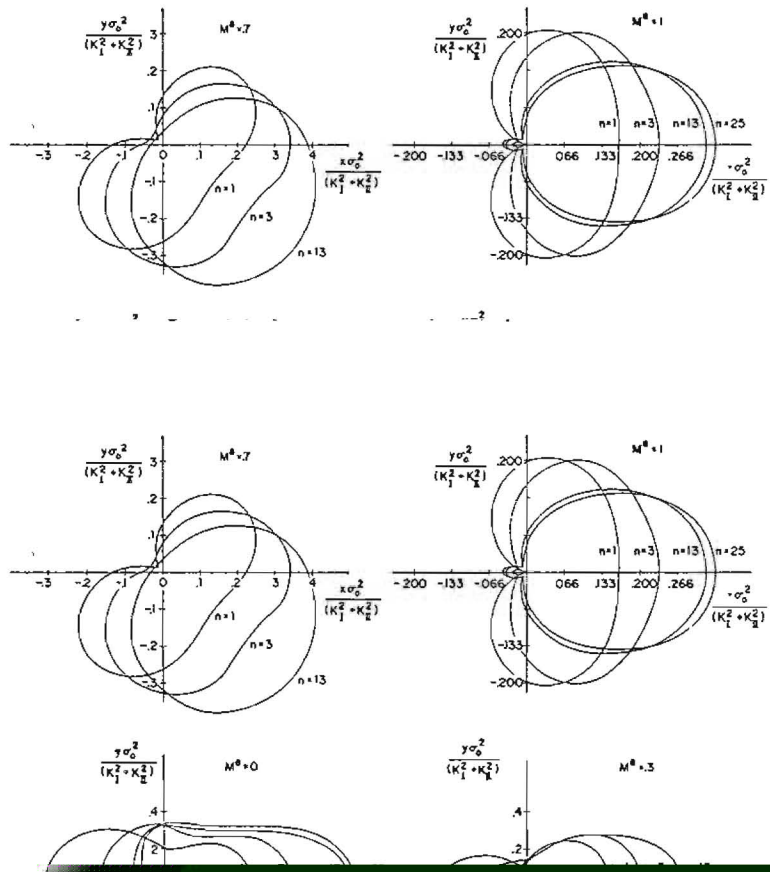


Fig. 5 θ^* (in degrees) as a function of M^e for small scale yielding. (a) plane stress, (b) plane strain.



REFERENCES

- [1] J. W. Hutchinson, J. Mech. Phys. Solids 16, 13 (1968).
- [2] J. W. Hutchinson, Ibid. 16, 337 (1968).
- [3] J. R. Rice and G. F. Rosengren, Ibid. 16, 1 (1968).
- [4] C. F. Shih, Small scale yielding analysis of mixed mode plane strain crack problems, Harvard University Report DEAP S-1, May 1973.
- [5] J. R. Rice, "Fracture" (edited by H. Liebowitz) (Academic Press, New York, 1968, 3, 191).
- [6] C. F. Shih, Elastic-plastic analysis of combined mode crack problems, Ph.D. Thesis, Harvard University, 1973.
- [7] A. F. Liu, AIAA Paper No. 73-253 (1973).
- [8] L. P. Pook, Engng. Fract. Mech. 3, 205 (1971).
- [9] P. D. Hilton and J. W. Hutchinson, Ibid. 3, 435 (1971).